Field- and concentration-tuned scaling of a quantum phase transition in a magnetically doped semiconductor

E. Helgren,[1] L Zeng,[2] K. Burch,[3,4] D. Basov,[4] and F. Hellman[1]

[1]*Department of Physics, University of California Berkeley, Berkeley, California 94720, USA*

[2]*Material Science Program, University of California San Diego, La Jolla, California 92093, USA*

[3]*MST-CINT, Los Alamos National Laboratory, Los Alamos, New Mexico 87545, USA*

[4]*Department of Physics, University of California San Diego, La Jolla, California 92093, USA*

Scaling analysis was performed on families of DC and AC conductivity curves falling on the metallic and insulating sides of the metal-insulator transition in the amorphous magnetically doped semiconductor, a-Gd_xSi_{1-x}. The transport curves were obtained both as a function of discretely varying both the gadolinium dopant concentration, x, and separately by changing an applied magnetic field, H. Both tuning parameters result in correlation length exponents of $\nu=1$ and dynamical scaling exponents of $z=2$. Temperature-frequency results differ markedly as compared to previous work on the nonmagnetic analog a-Nb_xSi_{1-x}. Our data also indicate a broader than predicted parameter space showing quantum critical behavior, and a phenomenologically determined quantum critical line in the zero temperature x-H plane is presented. The results are explained in terms of a single tunable parameter, namely disorder.

I. INTRODUCTION

The metal insulator transition (MIT) in both doped crystalline semiconductors and amorphous metal semiconductor alloys has been intensely studied for many years. Similar experimental results emerge for both types of materials as one tunes these structurally different systems through the MIT using some tuning parameter, such as dopant concentration, pressure, or magnetic field, indicating universal underlying physics. In general the increased structural disorder in the amorphous alloys has the effect that the MIT occurs at much greater dopant concentrations in these systems as compared to their crystalline counterparts. A subsequent result is that this greatly enhanced dopant concentration leads to a significantly larger Fermi energy, E_F. Fundamentally this disorder driven phase transition is regarded as an example of a quantum phase transition (QPT), strictly speaking a $T=0$ phase transition. However, measurements of the material properties taken at low but finite temperature in parameter space proximal to the quantum critical (QC) point should be controlled by the QC dynamics.[1] The greater E_F in the amorphous metal semiconductor alloy samples as opposed to their crystalline counterparts, such as Si:P, results in a broader region of parameter space wherein one can potentially observe scaling effects and the dependence of numerous parameters on critical exponents in and around the quantum critical regime as demonstrated in results from the amorphous metal semiconductor, a-Nb_xSi_{1-x}.[2–4]

Here we report on scaling results for the amorphous metal semiconductor alloy, a-Gd_xSi_{1-x}. The magnetic dopant Gd is trivalent, and has a half-full f shell resulting in the magnetic moment $J=S=7/2$. Introduction of a magnetic dopant has prominent consequences on the behavior of the system, such as an extremely large negative magnetoresistance (MR), a characteristic, concentration-dependent temperature scale at which magnetic interactions between electrons and the magnetic ions becomes relevant (leading to the enormous −MR), magnetic-field-dependent anomalous optical conductivity (spectral weight is not conserved up to the Si band edge), and a magnetic susceptibility which follows a near-Curie law temperature dependence yet has a nonmonotonic Gd concentration dependence.[5–8] Certain indications of successful scaling as a function of magnetic field have been seen in a-Gd_xSi_{1-x} before, including Hall coefficient measurements and tunneling measurements of the electron density of states (DOS).[9,10] These measurements were successful due in large part to the extremely large response of the DC conductivity to an applied field, with the phenomenological result that a sample with fixed dopant concentration, falling on the insulating side of the MIT, can be tuned through the transition using an external magnetic field, resulting in a crossover from insulating to metallic behavior.

We report here on scaling results in a-Gd_xSi_{1-x} for a systematic and comparative investigation of both the concentration tuned and magnetic field tuned MIT. Experiments on correlated disordered systems undergoing a MIT show a wide range of values for the critical exponents ν and z.[11] We report finding a dynamic scaling exponent $z=2$ as determined from the magnetic field tuned optical conductivity data consistent with previous DC results. This further verifies the important result that for a single system, using two distinct tuning parameters, concentration and magnetic field, we find identical critical exponents of $\nu=1$ and $z=2$ in contrast to experimental findings for Si:B, where different critical exponents, corresponding to different universality classes, are found depending on whether the system was tuned via concentration or a magnetic field.[12,13] However, we also note dramatic differences in the temperature-frequency scaling of a-Gd_xSi_{1-x} as compared to the nonmagnetic analogous system, a-Nb_xSi_{1-x}, and discuss a possible reason for this discrepancy.[3] These results all indicate that the scaling exponents come from the analysis of quantum critical (QC) dy-

namics near a QPT; however, we also argue that (using the conventional definition for the dimensionless distance over which scaling behavior is expected) the parameter space over which QC dynamics are observed seems to be larger than theory predicts.[13,14]

II. EXPERIMENT

Samples of amorphous Gd_xSi_{1-x} across a narrow range of dopant concentrations about the MIT were made by electron beam coevaporation at a base pressure of 10^{-9} Torr onto a parallel array of SiN-coated Si substrates (for measuring DC conductivity) and high resistivity silicon substrates (for optical measurement purposes) held at or below 70 °C. Film thicknesses were approximately 4000 Å with the thicknesses determined by profilometry. Rutherford backscattering verified the thicknesses and was used to determine the film concentrations relative to each other to an accuracy of ±0.2 at. %. Further details on sample preparation and characterization can be found in the literature.[6] DC conductivity data from room temperature to liquid helium temperatures were taken for all samples. By comparing these curves to previously studied samples close to the MIT, metallic samples, insulating samples, and a critical dopant concentration sample, $x_c=13.9$ at. %, were selected for further study. The magnetoconductivity of select samples was then measured in a He-3 charcoal sorption pump cryostat obtaining a base temperature of 400 mK in magnetic fields up to 8 tesla and these data are shown in Fig. 1. The optical magnetoconductivity measurements were performed on a Bruker IFS 66 v/S FTIR spectrometer coupled to an optical cryostat in a split coil superconducting magnet system capable of fields up to 8 tesla.[15] Transmission data in the FIR (0.3–3 THz) were obtained for the sample in a Faraday configuration, i.e., the magnetic field of the magnet perpendicular to the sample and the photon polarization (though since previous investigations showed no anisotropy in DC transport between parallel and perpendicular fields, either a Faraday or Voigt configuration could have been used).[9] Measurements taken with 0.25 cm^{-1} resolution resulted in transmission showing Fabry-Perot-like resonances (multiple internal reflections) which allows one to extract both the real and imaginary components of the complex frequency dependent optical conductivity.[4] The absolute transmission as determined from the optical measurements for this two-layer system (substrate plus thin film) at 0, 4.5, and 8 tesla is shown in Fig. 2. As described below, these fields correspond to insulating, critical, and metallic behavior as determined from the DC conductivity results. This spectral range allows for direct comparison with successful QC scaling results on a-Nb_xSi_{1-x} found in the literature.[3] Optical measurements were taken below 10 K to remain in what we refer to as the quantum limit, i.e., $\hbar\omega > k_BT$.

Figure 1(a) shows a family of magnetoconductivity curves in fields ranging from 8 to 0 tesla (top to bottom) for a sample with dopant concentration $x=13.7$ at. %. Across this range of magnetic fields, this one sample crosses over from displaying insulating to metallic behavior. In these systems, a metallic sample is defined as having a finite conduc-
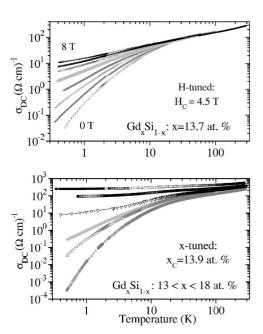

FIG. 1. The upper panel shows H-tuned magnetoconductivity for a single a-Gd_xSi_{1-x} sample for fields from 0 to 8 tesla. In zero field this sample lies on the insulating side of the MIT. The lower panel shows x-tuned DC conductivity curves for a range of dopant concentrations from 13 to 18 at. % Gd. Similar low temperature behavior for both x and H-tuned curves is noticeable. However, for the field tuned data, by 100 K, the effect of magnetic interactions on the DC transport has disappeared resulting in a convergence of the magnetotransport curves.

tivity, $\sigma_{DC}(T=0) \neq 0$, whereas an insulating sample has a conductivity that extrapolates to zero, $\sigma_{DC}(T=0)=0$. The conductivity of this insulating sample in an $8T$ field has a similar low temperature value as the metallic $x=14.3$ at. % sample in the zero field indicating that the sample in the field is well into the metallic regime. Figure 1(b) shows a family of DC conductivity curves for a-Gd_xSi_{1-x} samples spanning
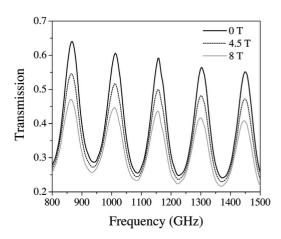

FIG. 2. Absolute optical transmission data taken at various magnetic fields for a-Gd_xSi_{1-x}. A series of Fabry-Perot-like resonances for this two-layer system (substrate+sample) are clearly discernible across this portion of the measured spectral range. As described in the text, these resonances allow for direct determination of both $\sigma_1(\omega)$ and $\varepsilon_1(\omega)$ of the sample.

a dopant concentration range of $x = 18.0$ to $x = 13.0$ at. % Gd, from the top to the bottom in the figure. These sets of data were chosen for attempted scaling since the critical magnetic field and dopant concentration fall in the middle of the family of curves. Note that the magnetoconductivity curves approach the $0T$ σ_{DC} curve by 100 K. This indicates that the mechanism allowing for tuning through the MIT at low temperatures near the QPT, have disappeared by this intermediate temperature; however, for samples tuned via concentration through the MIT, the curves are still distinct at 300 K.

III. RESULTS AND DISCUSSION

The continuous metal-insulator quantum phase transition allows for scaling analysis similar to that used in the study of continuous thermal phase transitions.[1,12–14,16,17] For a QPT, the DC conductivity can be written as follows:

$$\sigma_{DC}(g, T) = \frac{e^2}{\hbar \ell_T} f\left(\frac{\ell_T}{\xi_g}\right) \propto T^{1/z} f\left(\frac{|g - g_c|^{\nu}}{T^{1/z}}\right), \quad (1)$$

where $g \equiv x$, H is the tuning parameter, $\ell_T \propto T^{-1/z}$ is a thermal dephasing length[14] (a length scale over which an electron loses its quantum coherence), $\xi_g \propto |g - g_c|^{-\nu}$ is the correlation length on the metallic side or the localization length on the insulating side of the MIT, g_c refers to the critical value of the tuning parameter, and f is a generic function. Figure 3 shows the results of both x-tuned *and* H-tuned scaled DC conductivity data for a-Gd$_x$Si$_{1-x}$. In both cases the data show a similar collapse of metallic and insulating curves onto a generic functional form $f(\ell_T/\xi_g)$ as in the case of the nonmagnetic x-tuned analog a-Nb$_x$Si$_{1-x}$.[3] This is, however, an instance showing this type of scaling, which is a collapse of data, for the field tuned MIT in this class of materials. For both cases x and H, the metallic curves collapse on the functional form $f = 1 + (\ell_T/\xi_g)$ and the insulating curves $f = \exp[-(\ell_T/\xi_g)]$ are shown as solid lines in the figure.

The residual $T = 0$ conductivity, $\sigma_0 \propto (\xi_g)^{-1}$, for metallic curves, was used to determine the critical tuning parameter, $x_c = 13.9$ at. % or $H_c = 4.5T$ in the case of x or H field tuning, respectively. Further verification of the validity of x_c and H_c, followed from much poorer scaling using neighboring curves as the critical sample in trying to collapse the metallic and insulating curves.

The critical exponents were determined following analysis methods found in the literature.[2,18] On the metallic side of the MIT, σ_0 leads to a direct evaluation of the correlation length exponent, $\nu = 1$, again identical to x-tuned Nb-Si.[3] Analysis of the data in terms of variable range hopping (VRH) on the insulating side of the MIT has also been done. However, the resulting characteristic temperature, T_0 determined using the predicted form of Efros and Shklovskii (which includes electron-electron interactions) is inversely proportional to both the localization length and the dielectric constant, both of which diverge as a function of g approaching the MIT from the insulating side.[19] Thus an accurate determination of the localization length exponent ν from
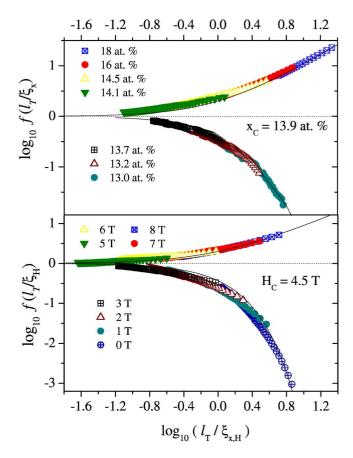

FIG. 3. (Color online) Results of scaling analysis for the dopant concentration tuned MIT (upper), and the magnetic field tuned MIT (lower) in a-GdSi. Analysis for both H- and x-tuned data results in $\nu = 1$ and $z = 2$. Both x-tuned and H-tuned metallic and insulating curves collapse onto the same functional form as described in the text.

insulating data requires an independent evaluation of the dielectric constant. However, T_0 decays as a power law as a function of $(g_c - g)$ for both x and H as one approaches the critical tuning parameter, i.e., approaching the QC point, from the insulating side and it is satisfying to note that the x_c and H_c that are approached as $T_0 \to 0$ closely match the values found from analysis of the metallic side and the "best collapse" criterion (see Fig. 3).

The real part of the complex optical conductivity, $\sigma_1(\omega)$, and the dielectric constant, $\varepsilon_1(\omega) = \varepsilon_\infty + 4\pi\sigma_2/\omega$ (where ε_∞ is the background dielectric constant and σ_2 is the imaginary part of the complex conductivity) for the a-Gd$_x$Si$_{1-x}$ sample that displayed successful H-tuned scaling is shown in Fig. 4. Both components are directly obtained from the structure in the transmission data as shown in Fig. 2 with no Kramers-Kronig (KK) calculation required. As explained in more detail in the literature, both components of the complex conductivity can be determined from the transmission data of this two-layer system (substrate+thin film) only after carefully characterizing the transmission through the substrate alone.[4] The structure in a two-layer transmission data is primarily determined by the 3 mm thick substrate, and shifts in
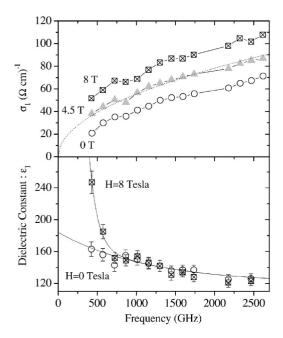
FIG. 4. Upper panel shows the optical conductivity taken for three different magnetic fields. The dotted line through the 4.5 tesla data is a fit using $\sigma_1(\omega) = A\omega^{1/2}$. The lower panel shows the magnetodielectric response, $\varepsilon_1(\omega, H)$, of the sample. The dotted lines are guides to the eye. In the limit of $\omega \to 0$, the insulating 0 tesla sample shows a tendency towards a finite dielectric constant whereas the dielectric constant of the metallic 8 tesla sample is divergent.

the peak height [mainly due to $\sigma_1(\omega)$] and center frequency [mainly due to $\varepsilon_1(\omega)$] come from the thin film sample. We find that both σ_1 and ε_1 are consistent with the KK compatible form for the complex optical conductivity, $\hat{\sigma} = \sigma_1 + i\sigma_2 = A(i\omega)^\alpha$ plus an additive residual conductivity term that is only dependent on the magnetic field.[16] The dielectric constant is expected to diverge as the transition is approached from the insulating side.[19] Though our experimental frequency range is far from the $\omega \to 0$ limit, and for most of this measured spectral range the magnetic field has no effect on ε_1, it is satisfying to note that the proper trend is seen in the low frequency end of the data, i.e., the insulating ($0T$) value is lower than the metallic ($8T$) value as indicated by the guides to the eye in the figure. We also point out that the frequency at which the magnetodielectric response turns on, i.e., where the $\varepsilon_1(\omega, H)$ data sets begin to deviate from each other, occurs at approximately 800 GHz, which, setting $\hbar\omega = k_B T$, is equivalent to 40 K. This is the same temperature at which the field dependent $\sigma_{DC}(T, H)$ data begins to deviate as well as seen in the upper panel of Fig. 1. Though no complete theory has emerged to describe the interactions between the magnetic moments and the conduction electrons in these amorphous magnetic semiconductor systems, the experimental evidence seems to indicate that screening and consequently the dielectric constant plays an important role.

Having measured the real part of the optical conductivity we are provided with an independent measure of the dynamic scaling exponent, z. At $g = g_c$ note the argument of f in
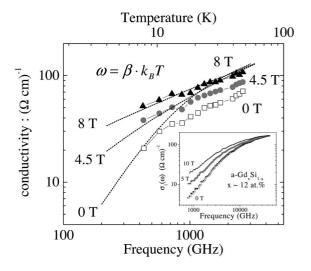

FIG. 5. This figure shows $\sigma_{DC}(T)$ (dotted lines) overlaid on the optical data $\sigma_1(\omega)$ (symbols), where the temperature and frequency axes have been scaled by $\pi h/1.25 k_B$. The inset shows optical conductivity data from another more insulating sample taken to higher frequency (Ref. 7). Only at the lowest temperature, i.e., when the frozen magnetic disorder is still present does the DC magneto-conductivity show marginal scaling with the optical magnetoconductivity.

Eq. (1) is 0, but the function must be analytic, so by setting it equal to unity, it follows then that $\sigma_{DC}(g_c, T) = e^2/\hbar \ell_T$. The dynamic scaling exponent z can be determined experimentally then from the functional dependence of the "best" critical conductivity curve. That is, a sample at x_c or H_c should show $\sigma_{DC} \propto T^{1/z}$, and indeed at low temperatures a-Gd$_x$Si$_{1-x}$ shows $\sigma_{DC} \propto T^{1/2}$ indicating $z = 2$. For photon energy $\hbar\omega \gg k_B T$, the optical conductivity would be analogously related to a frequency dependent dephasing length and should show $\sigma_1 \propto \omega^{1/z3}$. At the critical magnetic field, $H_C = 4.5$ tesla, we show in Fig. 4 that the data fits the following form, $\sigma_1(\omega) = A\omega^{1/2}$ as indicated by the dotted line. We therefore have independently determined that $z = 2$ from the optical data. This is shown in Fig. 5 which shows our experimental scaled H-tuned DC and AC transport data on a double logarithmic plot, in that the low energy optical excitations for the critical sample (solid gray circles; $H_c = 4.5T$) have an $\omega^{1/2}$ dependence. In summary, as found in a-Nb$_x$Si$_{1-x}$ for only the x-tuned MIT, we find for both the x and H-tuned sets of DC data, and from the field tuned optical data that $z = 2$, consistent with theoretical predictions for a system with interactions.[3,13] Due to the successful scaling (i.e., the identical collapse of the metallic and insulating curves) and the identical critical exponents for the x tuned and H tuned families of curves, we conclude that both x and H are in fact valid tuning parameters for this quantum phase transition.

Having established that both x and H tune the a-Gd$_x$Si$_{1-x}$ system through the QPT, we continue by comparing temperature-frequency scaling in the x-tuned a-Nb$_x$Si$_{1-x}$ case to our H-tuned a-Gd$_x$Si$_{1-x}$ results. For a-Nb$_x$Si$_{1-x}$, near unity temperature-frequency scaling was observed for an insulating, a critical, and a metallic sample.[3] Figure 5 shows

both the real part of the complex optical conductivity, $\sigma_1(\omega)$ (symbols), and $\sigma_{DC}(T)$ (dotted lines) for an a-Gd$_x$Si$_{1-x}$ sample, with $x=13.7$ at. % Gd, tuned with magnetic field through the MIT across identical temperature and frequency ranges as the study on a-Nb$_x$Si$_{1-x}$. However, the temperature frequency data do not collapse nearly as well as they do for a-Nb$_x$Si$_{1-x}$. The insulating, critical, and metallic curves for a-Gd$_x$Si$_{1-x}$ correspond to $0T$, $4.5T$, and $8T$, respectively. Setting $\hbar\omega=\beta\cdot k_B T$, the horizontal axes have been scaled by $\beta=\pi/1.25$ in order to (only marginally) visually collapse the lowest energy portions of the data. This approximate scaling value is also justified in that temperature-frequency scaling analysis in other instances has found similar scaling factors, i.e., a constant of order unity times the ratio $h\pi/k_B$.[3,20] Theory predicts this prefactor to be universal though,[14] and it is unclear to us what physical significance the differing prefactors represent.

The inset in Fig. 5 is magneto-optical data for a lower concentration, more insulating a-Gd$_x$Si$_{1-x}$ sample taken from the literature,[7] and is representative of all the magneto-optical data for a-Gd$_x$Si$_{1-x}$ taken to higher photon energy, namely that the magneto-optical conductivity curves merge at an energy scale of order 50 000 GHz. For $\sigma_{DC}(T,H)$ there is a clear energy scale at which the curves merge as well. The striking result is that the $\sigma_1(\omega,H)$ curves do not meet until much higher energy ($30T$ Hz ≈ 1000 K) as compared to the temperature at which the DC magnetoconductivity curves merge (40 K). Using this merging point to scale the temperature and frequency axes leads to a scaling factor $\beta=\pi/50$, inconsistent with previous temperature frequency scaling findings near a QPT. Attempts to scale the temperature and frequency using a nonlinear relation, i.e., $\omega\propto T^\alpha$ fails as well. This can actually be easily seen in that no scaling factor between ω and T could successfully make the data (specifically the merging point) collapse, because in fact the merging point for the DC data occurs at $100(\Omega$ cm$)^{-1}$, whereas for the optical data the extrapolated value where the various H-field curves would meet for a similar dopant concentration sample is $200(\Omega$ cm$)^{-1}$. From our results it is clear that the magnetically doped amorphous semiconductor system, upon tuning through the MIT with a magnetic field, does not show the same near unity temperature frequency scaling as was seen in the x-tuned case in a-Nb$_x$Si$_{1-x}$. A possible explanation for the differences between a-Gd$_x$Si$_{1-x}$ and the Nb doped nonmagnetic analog naturally lies in the magnetic interactions between the Gd ions and the charge carriers.

The magnetic ground state of a-Gd$_x$Si$_{1-x}$ (for $H=0$) is a spin glass, with the quenched magnetic disorder stemming from competing ferromagnetic and antiferromagnetic interactions between the magnetic dopant atoms.[8] As the temperature is increased to obtain $\sigma_{DC}(T)$, the frozen frustrated magnetic landscape "melts" reducing the magnetic disorder seen by diffusing electrons increasing the conductivity of a given sample (in fact it is the time scale of the magnetic moment fluctuations that decreases with increasing temperature). In the parlance of continuous quantum phase transitions, we may say that as the magnetic ground state melts, the chang-

ing magnetic correlation length becomes the dominant length scale in the system, and the electrons lose their quantum coherence, leading to the breakdown of the QC scaling. In contrast, for increasing photon energy, i.e., with increasing ω, the pairs of electronic sites contributing to absorption, continue to see the strong magnetic disordered potential landscape of the quenched magnetic moment orientation, which is indicated by the $\omega^{1/2}$ dependence seen across the entire measured frequency range in Fig. 5. A strong magnetic field changes the magnetic disorder potential landscape seen by the charge carriers as well, affecting both the low temperature DC and the entire measured range of the AC data similarly (for increasing H, unlike for T, the disorder actually vanishes as the moments become more aligned). This also explains the observed increase of the conductivity with increasing field, as the magnetic moments align more (very likely as a function of the reduced magnetization M/M_S).[21] However, M/M_S has been shown to still be much less than unity at 10 tesla in a-Gd$_x$Si$_{1-x}$,[22] thus we would expect H to tune the system through the QPT, though with decreasing efficiency, up to M_S. In fact M/M_S, may be the more appropriate tuning parameter, but up to 10 tesla, there is a near unity relation between H and M/M_S for a-Gd$_x$Si$_{1-x}$.

Having two separate controllable parameters in a single system that successfully tune through the QPT allows for unique insights into theoretical predictions for these $T=0$ phase transitions. Though critical exponents may be the same or at least similar to within experimental and theoretical uncertainty from one universality class to another, our initial expectation was that a magnetic field of a few tesla, usually considered quite strong by experimental standards, would be sufficient to push the system into a different universality class. Indeed as stated in their review, Belitz and Kirkpatrick claim that the analogous system a-NbSi, falls in the spin-orbit (SO) universality class, and that such systems, when placed in a strong magnetic field cross over to the magnetic impurity (MI) universality class, with distinctly different expected values of the dynamic scaling exponent, z.[13] The fact that z is the same for both x and H tuning, may be explained in one of two ways. First, since Gd has a strong magnetic moment, the system may originally fall into the MI class (this seems the more obvious choice given the nature of the Gd dopant ions) and remain there throughout the parameter space of concentrations and magnetic fields that were used. However, for both methods of tuning through the MIT we find $z=2$, but for the MI universality class, $z>2$ is expected. Second, if indeed a-Gd$_x$Si$_{1-x}$ falls into the SO class like a-NbSi (for which $z=2$ is expected), then the somewhat striking result that the x and H tuned critical exponents are the same may also be accounted for by the fact that the magnetization is still far from being saturated, and that the applied fields are not strong enough to push the system into another universality class.

Theoretical predictions for the range of parameter space over which QC behavior can be seen near the MIT state that the following inequality for the dimensionless distance from the MIT need apply: $\delta\equiv|g-g_c|/g_c\lesssim 0.1$, where g is the tuning parameter (i.e., x or H in our case) and g_c is the critical
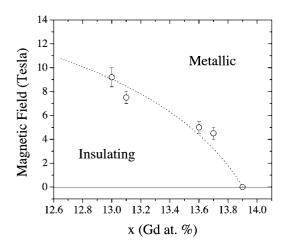
FIG. 6. Phase boundary, or quantum critical line, in the zero temperature x-H plane, that separates metallic and insulating behavior in a-Gd_xSi_{1-x}.

value.[13] Our experimental range for δ over which we observe scaling for the x and H tuned data varies quite dramatically. For instance on the insulating side of the MIT for concentration tuning, using the extreme case, $x=13.0$ at. % and $x_c=13.9$ at. %, we find $\delta=0.07$, well within the acceptable theoretical limit. However, the opposite extreme occurs for the results on the insulating side of the field driven family of curves, which results in $\delta=1$, using $H=0T$ and $H_c=4.5T$. Other experimental evidence of scaling for regions larger than $\delta \leqslant 0.1$ exist.[23,24] However, it is interesting to note that the change in the magnitude of the low temperature value of $\sigma_{DC}(T)$ for the $\delta=1$ H-field tuned case, i.e., from 0 to $4.5T$, corresponds to changing the concentration of the system from $x=13.7$ at. % to $x_c=13.9$ at. %, a much smaller equivalent δ. Thus though both the concentration and the magnetic field can be used to effectively tune through the MIT, that is each separately changes the disorder of the system in a unique manner, the dimensionless distance δ as defined above is not a good indicator of the QC parameter space. The true tuning parameter for this QPT is disorder which apparently has nonequivalent dependencies on x and H as seen by the relative change in $\sigma_{DC}(T)$ for equivalent changes in δ, (e.g., $\delta=0.02$). This dramatic difference in dimensionless distance from the MIT for corresponding changes in the conductivity indicates that this criterion warrants closer inspection.

A subsequent result of our investigation of the x and H-field tuned MIT in a-Gd_xSi_{1-x} is shown in Fig. 6. Having measured numerous samples near the MIT, and drawing upon previous results, we have determined a phenomenological quantum critical line, i.e., a collection of quantum critical points, in the zero-temperature x-H plane in the phase space for our system. H_c and the error bars shown in the figure come from analysis of the field tuned families of low temperature $\sigma_{DC}(T)$ curves. The residual conductivity was analyzed for more metallic samples and the characteristic VRH temperature was analyzed for more insulating samples, each of which converge to zero at the MIT. This phase

boundary, we believe, must be a representation of the critical disorder boundary, tunable via either dopant concentration or magnetic field, for this QPT. However, the error bars indicate not only a measure of the systematic error in the determination of H_c, but also the possible existence of slight variations in the local DOS very close to the Fermi energy which become more pronounced so close to the MIT. This subtle inhomogeneity may cause a blurring of the otherwise sharp phase transition, consistent with recent reports on measurements examining the parameter space very close to the transition.[25]

IV. CONCLUSION

Our system, a-Gd_xSi_{1-x}, shows evidence of strong electron correlations, a high degree of disorder and complex magnetic interactions, both between the ionic magnetic moments themselves (resulting in the spin glass ground state) and between the conduction electrons and the Gd moments, as indicated by the extremely large negative MR and x-dependent characteristic onset temperature.[6] Thus, though this system is similar to the intensely studied manganites and dilute magnetic semiconductors systems, like GaMnAs, there is no all-encompassing theory that sufficiently accounts for magnetic interactions, electron correlations, and disorder. The benefit of utilizing scaling analysis on this system is that successful scaling is independent of the underlying physics in the quantum critical regime. Here from our temperature frequency scaling results we observe the breakdown of QC scaling either entirely or potentially at a much lower thermal or photon energy scales than that seen in a-Nb_xSi_{1-x}. Further investigations to lower photon energy (i.e., below 300 GHz), but still in the quantum limit (i.e., $k_BT < \hbar\omega$), though extremely difficult from an experimental standpoint, would be needed to shed light on whether temperature-frequency scaling works in a-Gd_xSi_{1-x} at all. Since the major difference between these two systems stems from the magnetic nature of the dopant Gd, we believe that we are observing this breakdown in scaling due to some change in the local moment of the system and subsequent change in the interaction between the local moments and the current carrying electrons. The breakdown of QC scaling seen here has allowed us to deduce important physical processes in these magnetically doped amorphous semiconductor systems and hopefully will provide impetus for continued theoretical study.

In summary, we have shown successful scaling of both x tuned and H tuned data near the MIT for a single system by discretely varying the magnetic dopant concentration or the magnetic field. The identical critical exponents, even up to externally applied magnetic fields of 8 tesla suggest that the system remains in a single universality class, perhaps because M/M_S is still relatively small (~ 0.3) at this applied field. We also find that QC dynamics persist to a much broader parameter space than expected. The low energy electrodynamics of this system, as probed via the real part of the optical conductivity, show an independent determination of the scaling exponent as $z=2$, consistent with previous dc

transport data on a-Gd_xSi_{1-x} and a further link to the non-magnetic analog a-Nb_xSi_{1-x}. However, we find a distinct breakdown of temperature frequency scaling in an identical energy range over which successful near unity temperature frequency scaling was seen in a-Nb_xSi_{1-x}. A simple model explaining the breakdown in scaling for the magnetically doped system in terms of the variations in the Gd moment potential landscape as seen by diffusing electrons is presented. Our data also allow us to determine a phenomeno- logical phase boundary line, or quantum critical line, in the zero temperature x-H plane.

[1] S. Scahdev, *Quantum Phase Transitions* (Cambridge University Press, New York, 1999).

[2] G. Hertel, D. J. Bishop, E. G. Spencer, J. M. Rowell, and R. C. Dynes, Phys. Rev. Lett. **50**, 743 (1982).

[3] H.-L. Lee, J. P. Carini, D. V. Baxter, W. Henderson, and G. Gruner, Science **287**, 633 (2000).

[4] E. Helgren, G. Gruner, M. R. Ciofalo, D. V. Baxter, and J. P. Carini, Phys. Rev. Lett. **87**, 116602 (2001).

[5] F. Hellman, M. Q. Tran, A. E. Gebala, E. M. Wilcox, and R. C. Dynes, Phys. Rev. Lett. **77**, 4652 (1996).

[6] E. Helgren, J. J. Cherry, L. Zeng, and F. Hellman, Phys. Rev. B **71**, 113203 (2005).

[7] D. N. Basov, A. M. Bratkovsky, P. F. Henning, B. Zink, F. Hellman, Y. J. Wang, C. C. Homes, and M. Strongin, Europhys. Lett. **57**, 240 (2002).

[8] F. Hellman, D. R. Queen, R. M. Potok, and B. L. Zink, Phys. Rev. Lett. **84**, 5411 (2000).

[9] W. Teizer, F. Hellman, and R. C. Dynes, Phys. Rev. B **67**, 121102(R) (2003).

[10] W. Teizer, F. Hellman, and R. C. Dynes, Phys. Rev. Lett. **85**, 848 (2000).

[11] E. Abrahams and G. Kotliar, Science **274**, 1853 (1996).

[12] S. Bogdonavich, M. P. Sarachik, and R. N. Bhatt, Phys. Rev. Lett. **82**, 137 (1999).

[13] D. Belitz and T. R. Kirkpatrick, Rev. Mod. Phys. **66**, 261 (1994).

[14] S. L. Sondhi, S. M. Girvin, J. P. Carini, and D. Shahar, Rev. Mod. Phys. **69**, 315 (1997).

[15] W. J. Padilla, Z. Q. Li, K. S. Burch, Y. S. Lee, K. J. Mikolaitis, and D. N. Basov, Rev. Sci. Instrum. **75**, 4710 (2004).

[16] E. Helgren, N. P. Armitage, and G. Gruner, Phys. Rev. B **69**, 014201 (2004).

[17] F. J. Wegner, Z. Phys. **25**, 327 (1976).

[18] W. Teizer, F. Hellman, and R. C. Dynes, Solid State Commun. **114**, 81 (2000).

[19] A. L. Efros and B. I. Shklovskii, in *Electron-Electron Interactions in Disordered Systems*, edited by A. L. Efros and M. Pollak (Elsevier, New York, 1985), pp. 409–482.

[20] L. W. Engel, D. Shahar, C. Kurdak, and D. C. Tsui, in *Proceedings of the 11th International Conference on High Magnetic Fields in the Physics of Semiconductors*, edited by D. Heiman (World Scientific, Singapore, 1995), p. 236.

[21] J. M. D. Coey, M. Viret, and S. von Molnar, Adv. Phys. **48**, 267 (1999).

[22] F. Hellman, W. Geerts, and B. Donehew, Phys. Rev. B **67**, 012406 (2002).

[23] P. Dai, Y. Zhang, and M. P. Sarachik, Phys. Rev. B **45**, 3984 (1992).

[24] T. F. Rosenbaum, R. F. Milligan, M. A. Paalanen, G. A. Thomas, R. N. Bhatt, and W. Lin, Phys. Rev. B **27**, 7509 (1983).

[25] L. Bokacheva, W. Teizer, F. Hellman, and R. C. Dynes, Phys. Rev. B **69**, 235111 (2004).